# First-principles study of the influence of (110)-oriented strain on the ferroelectric properties of rutile $TiO_2$

A. Grünebohm,[1,*] C. Ederer,[2] and P. Entel[1]

[1]*Faculty of Physics and Center for Nanointegration, CeNIDE, University of Duisburg-Essen, D-47048 Duisburg, Germany*

[2]*School of Physics, Trinity College, Dublin 2, Ireland*

(Received 14 June 2011; revised manuscript received 7 October 2011; published 28 October 2011)

We use first-principles density-functional theory to investigate the softening of polar phonon modes in rutile $TiO_2$ under tensile (110)-oriented strain. We show that the system becomes unstable against a ferroelectric distortion with polarization along (110) for experimentally accessible strain values. The resulting polarization, estimated from the Born effective charges, even exceeds the bulk polarization of $BaTiO_3$. Our calculations demonstrate the different strain dependence of polar modes polarized along (110) and (001) directions, and we discuss the possibility of strain engineering the polarization direction, and the resulting dielectric and piezoelectric response, in thin films of $TiO_2$ grown on suitable substrates.

DOI: 10.1103/PhysRevB.84.132105 PACS number(s): 77.22.−d, 77.80.bn, 77.84.−s

Rutile $TiO_2$ is an *incipient* ferroelectric material,[1,2] and it has been shown via *ab initio* simulations that a ferroelectric transition can be induced by either negative pressure or (001)-oriented strain.[3–6] An experimental realization of ferroelectric $TiO_2$ would have great technological impact, since this material is cheap and optimized processing techniques are readily available. $TiO_2$ is currently used for a large variety of applications such as solar cells or pigments. Besides, due to its high dielectric constant ($\epsilon = 251$ at low temperatures[7]), $TiO_2$ is also used in dielectric devices. Hence the possibility to tune the electric permittivity with or without inducing a ferroelectric transition would be of great technological importance.

Most applications are based on the (110) surface, which can be strained in either the $(\bar{1}10)$ or (001) direction by growth on a suitable substrate. Until now, only the influence of isotropic and (001)-oriented strain on a ferroelectric state with polarization along (001) has been investigated for bulk rutile.[3,5,6,8] The resulting ferroelectricity can be attributed to the only polar phonon mode polarized in the (001) direction, $A_{2u}$, which softens if the Ti-O distances are enlarged. Interestingly, it was predicted recently that the $A_{2u}$ mode is insensitive to (110) strain whereas an acoustic phonon mode softens under these strain conditions.[8] Apart from $A_{2u}$, rutile possesses additional low-energy phonon modes, which are polarized along (110), and for which a detailed understanding is still missing.

Here, we investigate the role of (110)-oriented strain on the ferroelectric properties of rutile $TiO_2$.[9] The main goal of our work is a systematic investigation of the influence of (110) strain on polar modes in the (001) and (110) directions. We show that the paraelectric state of rutile is destabilized under tensile strain and a polarization along (110) is induced. Furthermore, a polarization in (001) direction can be obtained if the ionic shifts along the (110) direction are suppressed.

All results presented here are obtained from self-consistent density-functional theory calculations employing the "Vienna Ab Initio Simulation Package" (VASP 5.2.2)[10] with a plane-wave basis, projector augmented wave potentials,[11] and the generalized gradient approximation (GGA) in the formulation of Perdew, Burke, and Ernzerhof.[12] For Ti (O) atoms the $4s3d$ ($2s2p$) electrons are treated as valence. Ionic positions are optimized until all forces are smaller than 0.01 eV/Å and a $\sqrt{2} \times \sqrt{2} \times 1$ supercell containing 4 $TiO_2$ units, see Fig. 1, is used. A plane-wave cutoff of 500 eV and a sampling of the Brillouin zone with a $5 \times 11 \times 5$ Monkhorst-Pack mesh[13] guarantee a high accuracy of the simulations. Born effective charges have been calculated using density-functional perturbation theory.[14]

The rutile crystal structure of $TiO_2$ is tetragonal with space group symmetry $P4_2/mnm$ [see the primitive unit cell inserted in Fig. 1(c)]. Each Ti-atom is sixfold coordinated by O atoms, with four short *equatorial* Ti-O bonds and two longer *apical* bonds; see Fig. 1(b). The exact Ti-O distances are determined by the lattice constant $a$, the tetragonal $c/a$ ratio, and the internal structural parameter $u$. From our relaxations we obtain $a = 4.6640$ Å (4.587 Å), $c/a = 0.6366$ (0.644), and $u = 0.3047$ (0.305). For comparison, experimental results from Ref. 15, using neutron diffraction at 15 K, are given in brackets.

As mentioned in the Introduction, one polar optical $A_{2u}$ mode with polarization along (001) exists in rutile. The corresponding ferroelectric state can be stabilized by increasing the equatorial Ti-O bond length, since this reduces the short-range repulsion between the two ions.[3–5] Furthermore, there are three pairs of doubly degenerate polar optical phonon modes of $E_u$ symmetry, which correspond to atomic displacements within the (110)-$(\bar{1}10)$ plane.[1] In Ref. 3 it has been shown that a uniform lattice expansion causes a softening of the energetically lowest $E_u$ mode, although this effect is smaller than the corresponding change for the $A_{2u}$ mode.

The application of (110) strain reduces the symmetry to the orthorhombic space group $Cmmm$, with two inequivalent Ti ($Ti_1$,$Ti_2$) and O ($O_1$, $O_2$) sublattices. The imposed strain changes the *apical* $Ti_1$-$O_2$ and the *equatorial* $Ti_2$-$O_2$ bond distance, whereas the *equatorial* $Ti_1$-$O_1$ and the *apical* $Ti_2$-$O_1$ bonds are not modified; see Fig. 1(a). As a result, the twofold degeneracies among the six optical $E_u$ modes are lifted and they split into three $B_{2u}$ and three $B_{3u}$ modes with atomic shifts along $(\bar{1}10)$ and (110), respectively.

For further analysis of the atomic displacements it is convenient to decompose the $3 \times N$ dimensional displacement vector $\mathbf{Y}$ into a linear combination of three mode patterns $\mathbf{B}_{3u,i}$

 

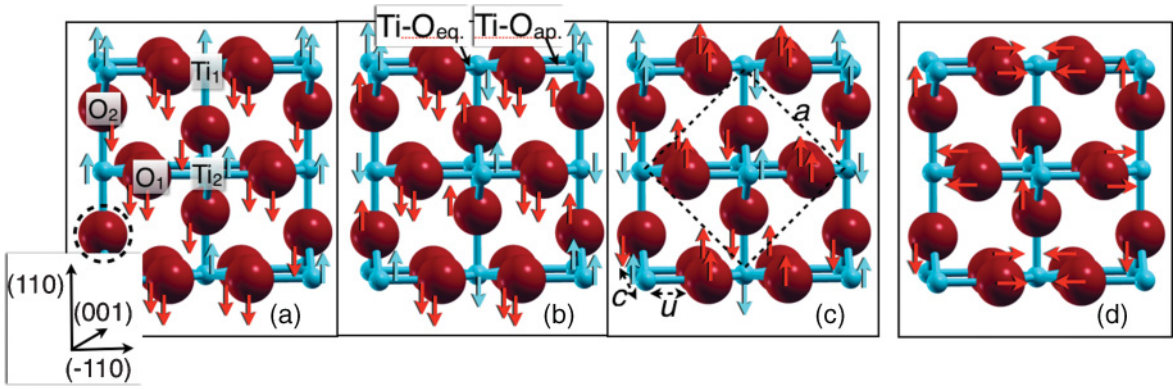


FIG. 1. (Color online) Atomic structure of bulk rutile in the $\sqrt{2} \times \sqrt{2} \times 1$ supercell. (a)–(c) Solid arrows indicate the atomic shifts for the three (110) polarized $B_{3u}$ modes used in our analysis, sorted in ascending order of their energies. (a) $B_{3u,1}$ mode; indices mark inequivalent Ti/O sublattices under (110) strain, and the dotted circle marks the O atom, which has been shifted previous to the structural optimization; (b) $B_{3u,2}$ mode; (c) $B_{3u,3}$ mode. Dotted lines and arrows mark the primitive unit cell, the lattice constants $a$ and $c$, and the internal structural parameter $u$. (d) Additional superimposed displacements in the fully relaxed state (corresponding to $\mathbf{R}$).

and an additional relaxation $\mathbf{R}$,

$$\mathbf{Y} = A \cdot \mathbf{B}_{3u,1} + B \cdot \mathbf{B}_{3u,2} + C \cdot \mathbf{B}_{3u,3} + \mathbf{R}. \quad (1)$$

Here, $N$ is the number of atoms within the supercell. We use a set of $B_{3u,i}$ modes with displacement patterns as sketched in Fig. 1(a)–1(c) and the same magnitude of displacements on all sublattices. These three modes, together with the corresponding acoustic mode, form a complete basis for representing the $B_{3u}$ eigenmodes of the strained rutile structure. Since we are only interested in the three optical modes, we do not consider the acoustic mode in our analysis. We note that even though the displacement amplitudes of the various sublattices in the exact phonon eigenvectors cannot be fully determined by symmetry arguments alone, the three mode vectors depicted on Fig. 1 are indeed relatively close to the actual $E_u$ eigenvectors of unstrained $TiO_2$.

To explore the energy landscape of (110)-strained $TiO_2$ as function of the $B_{3u}$ optical modes, we perform total-energy calculations with fixed atomic positions, and include different amounts of the three distortion modes $B_{3u,i}$. The system is softest along $B_{3u,1}$, but a combination of $B_{3u,1}$ and $B_{3u,2}$ is required to produce a stable ferroelectric energy minimum; see Fig. 2. This energy minimum is shifted to larger amplitudes for increasing strain [compare Figs. 2(a) and 2(b)], but no major differences appear for higher strain values. In the following we focus our discussion on the case of 2% strain.

In order to locate an approximate energy minimum, we first identify the most favorable $B_{3u,2}$ amplitude as a function of $B_{3u,1}$, and then vary the amplitude of $B_{3u,3}$ for the resulting optimal linear combinations of $B_{3u,1}$ and $B_{3u,2}$. The so-obtained energy landscape is shown in Fig. 2(c). From this we derive an approximate energy minimum at $\mathbf{Y}_0$ corresponding to $A = 0.096$ Å, $B = 0.035$ Å, $C = 0.017$ Å, and $\mathbf{R} = 0$.

The results of our full structural relaxations for different magnitudes of (110) strain are listed in Table I. The symmetry of the system has been reduced to $Pmm2$ prior to the relaxation by shifting one of the $O_2$ atoms 0.002 Å along (110); see Fig. 1(a).

The atomic relaxations confirm that for tensile (110) strain the paraelectric state is destabilized by a polar shift of the sublattices against each other in the (110) direction. This shift, which is well approximated by $\mathbf{Y}_0$ (see Table I), leads to alternating expansion/contraction of the short $Ti_2$-$O_2$ bonds. However, since a further increase of this bond length (besides the increase resulting from the overall (110) strain) is unfavorable, additional atomic displacements ($\mathbf{R}$) corresponding to an $M$ point zone-boundary mode lead to different (110) shifts of the two $O_2$ atoms; see Fig. 1(d). Furthermore, a small relaxation of the $O_1$ atoms in the $(\bar{1}10)$ direction (not included in Table I) is also superimposed to $\mathbf{Y}_0$; see Fig. 1(d). As a result, the $Ti_1$-$O_1$ bond length is approximately conserved, even though these ions are shifted against each other in the (110) direction. This lowers the energy for the (110) shift and thus the amplitudes of the (110) shift for these sublattices are slightly increased compared to $\mathbf{Y}_0$.

The resulting spontaneous polarization can be estimated by

$$P_{(110)} = \frac{1}{V} \sum_i x(i) \cdot Z^*_{(110),i}. \quad (2)$$

Here, the summation is over all atoms in the unit cell with volume $V$, $x(i)$ represents the shift of atom $i$ in the (110) direction, and $Z^*_{(110),i}$ is the corresponding principal value of the Born effective charge tensor for undistorted bulk. As the Born charges in $TiO_2$ are quite stable with respect to small modifications of the Ti-O distances,[6] this approximation is sufficient for a qualitative discussion. We obtain $Z^*_{(110)} = 7.59|e|$ $(-5.14|e|)$ for $Ti_1$ $(O_2)$, which has the apical bond

TABLE I. Amplitudes $x$ (in Å) of atomic shifts in (110) direction under tensile strain. The energy differences $\Delta E$ relative to the paraelectric state at the same strain are given in meV/$TiO_2$ unit, and the resulting polarization $P_s$ in $\mu C/cm^{-1}$.

| Strain | $x(Ti_1)$ | $x(Ti_2)$ | $x(O_1)$ | $x(O_2)$ | $\Delta E$ | $P_s$ |
|---|---|---|---|---|---|---|
| 1.02[a] | 0.09 | 0.04 | −0.02 | −0.04 | 4.8 | 33 |
| 1.02 | 0.10 | 0.04 | −0.03 | −0.03/−0.05 | 6.0 | 35 |
| 1.03 | 0.13 | 0.05 | −0.03 | −0.04/−0.08 | 15.2 | 46 |
| 1.04 | 0.16 | 0.05 | −0.03 | −0.04/−0.10 | 29.8 | 54 |
| 1.05 | 0.19 | 0.05 | −0.03 | −0.05/−0.13 | 49.3 | 62 |

[a]Shift along $\mathbf{Y}_0$ without further atomic relaxation.

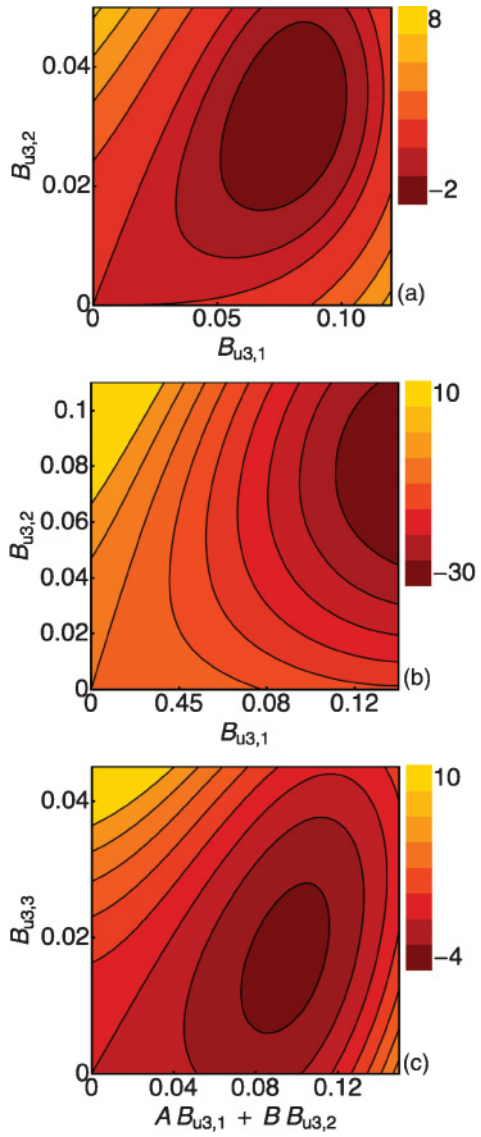


FIG. 2. (Color online) Energy landscapes for static displacements along the $B_{3u,i}$ mode vectors corresponding to 2% strain (a),(c) and 5% strain (b). Amplitudes of the modes are given in Å and energies in meV/$TiO_2$ unit relative to the unrelaxed strained configuration.

aligned along (110), whereas we obtain $Z^*_{(110)} = 5.35|e|$ $(-1.32|e|)$ for $Ti_2$ $(O_1)$, which is in qualitative agreement with $Z^*_{(110)} = 7.34|e|$ $(-4.98|e|)$ along the *apical* bond, respectively $Z^*_{(110)} = 5.34|e|$ $(-1.36|e|)$ for the perpendicular direction obtained by Lee *et al.*[1]

With Eq. (2) we calculate a sizable polarization, which is already in the technical relevant range for a strain of 2%; see Table I. The resulting ferroelectric state is 6 meV/formula unit lower in energy than the paraelectric state. If one assumes that the ferroelectricity is related to exactly one degree of freedom at the Γ point this corresponds to a thermal energy of about 139 K. However, since the depth of the energy well increases strongly with the imposed strain, a ferroelectric phase should be experimentally accessible for about 5% tensile strain as our rough estimation already results in a thermal energy of 1146 K in this case.

For compressive (110) strain, the reduction of the Ti-O distances induces a large short-range repulsion, and a ferroelectric distortion is unfavorable. Instead, $O_2/O_1$ atoms increase the $(110)/(\bar{1}10)$ component of their *equatorial* bond, due to the larger compressibility of the *apical* bond. This is in agreement with the hardening of the ferroelectric $A_{2u}$ mode under compression.[3,6]

We note that we could not reproduce the destabilization of the system along an acoustic phonon mode under (110) strain found in Ref. 8, for which an energy gain of several meV has been predicted, even if we use a $2 \cdot \sqrt{2} \times 2 \cdot \sqrt{2} \times 4$ supercell, which is commensurable with the displacement pattern of this mode. Additionally, we do not find imaginary frequencies of the $A_{2u}$mode, contrary to earlier studies based on GGA potentials.[4,8] Possible explanations for these discrepancies are the different potentials used and the resulting difference in lattice parameters.

Finally, we discuss the relationship between the polar modes with polarization along (110) and (001), respectively. Since the *equatorial* Ti-O bond length increases under tensile (110) strain, the short-range repulsion between these ions is reduced, and a polar shift along (001) should become likely. Nevertheless, no softening of the $A_{2u}$ mode under (110) strain has been observed in previous *ab initio* investigations.[8] In contrast, our calculations show that the polar mode in the (001) direction can be stabilized if the displacements along the $B_{3u}$ modes are suppressed; see Fig. 3.[16] If the ions are not

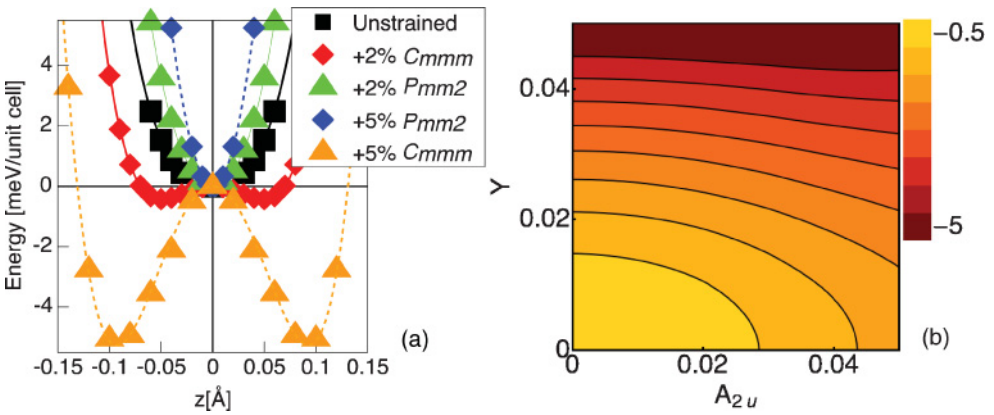


FIG. 3. (Color online) (a) Total-energy change for static atomic displacements along the $A_{2u}$ mode under uniaxial (110) strain for atomic positions relaxed with imposed $Cmmm/Pmm2$ symmetry. Here, only the second symmetry class allows for polarization in (110) direction. (b) Energy landscape for mixed displacements along $\mathbf{Y}_0$ and $A_{2u}$ for 2% tensile strain in (110) direction.

allowed to displace along (110), a characteristic double well potential appears for tensile (110) strain, and the well depth increases with increasing strain. However, a coupling between soft modes corresponding to (110) and (001) polarization exists, similar to perovskites such as, e.g., $SrTiO_3$.[17] As a result, the ferroelectric mode polarized in the (110) direction disables polar distortions in the (001) direction. If the strain increases from 2% to 5%, and the relative ionic shifts in the (110) direction increase, more energy is needed to shift the sublattices relative to each other along (001). Figure 3(b) shows the energy landscape as a function of polar shifts along (001), $A_{2u}$, and along the optimized mode vector $\mathbf{Y}_0$ in the (110) direction.

While for pure (110)-oriented strain the energy gain corresponding to the $A_{2u}$ mode is one order of magnitude smaller than the energy gain corresponding to $B_{3u}$, a further softening occurs under tensile (001) strain,[3] which is stronger for $A_{2u}$ than for $B_{3u}$. The exact location and depth of the energy minimum within the "$A_{2u}$-$B_{3u}$ plane" can therefore be adjusted by straining in both (110) and (001) directions, which can be achieved in thin films by choosing an appropriate substrate. This opens up the exciting possibility of "strain engineering" the polarization direction in $TiO_2$, and the resulting dielectric and piezoelectric response, similar to the case of perovskite ferroelectrics.[17,18]

In summary, we have shown that a ferroelectric state can be stabilized in rutile under tensile (110)-oriented strain. The main contribution of the displacement pattern can be attributed to the $E_u$ phonon modes of undistorted rutile. For 5% strain a large polarization of 63 $\mu C/cm^{-1}$ emerges in the (110) direction. The depth of the corresponding energy well is large in comparison to thermal fluctuations at low temperatures, which suggests that the ferroelectric state can indeed be observed experimentally. We note that while the well-known small overestimation of unit-cell volumes within GGA may also slightly overestimate the tendency toward ferroelectric distortions, qualitative trends are nevertheless described properly and agree well with other calculations.[4,6,19]

Furthermore, we have demonstrated that a ferroelectric state in the (001) direction can also be stabilized under tensile (110) strain, if the polar shifts along the (110) direction are suppressed. This indicates a coupling between optical modes polarized in (001) and (110) directions, which allows to shift the relative energies of ferroelectric states with polarization in (110) and (001) directions under different strain conditions. Future investigations are necessary in order to investigate the influence of additional (001) strain on the ferroelectric modes in more detail. In addition, the effect of surface-induced atomic relaxations at the real (110) surface on the polar phonon modes is important and will be addressed in an upcoming investigation.[6]

This work was supported by the Deutsche Forschungsgemeinschaft (Grant No. SFB 445) and by Science Foundation Ireland (Grant No. SFI-07/YI2/I1051).

*anna@thp.uni-duisburg.de

[1] C. Lee, P. Ghosez, and X. Gonze, Phys. Rev. B **50**, 13379 (1994).
[2] J. G. Traylor, H. G. Smith, R. M. Nicklow, and M. K. Wilkinson, Phys. Rev. B **3**, 3457 (1971).
[3] B. Montanari and N. M. Harrision, J. Phys.: Condens. Matter **16**, 273 (2004).
[4] B. Montanari and N. M. Harrision, Chem. Phys. Lett. **364**, 528 (2002).
[5] Y. Liu, L. Ni, Z. Ren, G. Xu, C. Song, and G. Han, J. Phys.: Condens. Matter **21**, 275901 (2009).
[6] A. Grünebohm, C. Ederer, and P. Entel (unpublished).
[7] G. A. Samara and P. S. Peercy, Phys. Rev. B **7**, 1131 (1973).
[8] P. D. Mitev, K. Hermansson, B. Montanari, and K. Refson, Phys. Rev. B **81**, 134303 (2010).
[9] Unlike in epitaxial strain calculations, we impose strain in one direction only and no further optimization of the cell shape is performed.
[10] G. Kresse and J. Furthmüller, Phys. Rev. B **54**, 11169 (1996).
[11] P. E. Blöchl, Phys. Rev. B **50**, 17953 (1994).
[12] J. P. Perdew, K. Burke, and M. Ernzerhof, Phys. Rev. Lett. **77**, 3865 (1996).
[13] H. J. Monkhorst and J. D. Pack, Phys. Rev. B **13**, 5188 (1976).
[14] M. Gajdoš, K. Hummer, G. Kresse, J. Furthmüller, and F. Bechstedt, Phys. Rev. B **73**, 045112 (2006).
[15] J. K. Burdett, T. Hughbanks, and J. Gordon, J. Am. Chem. Soc. **109**, 3639 (1987).
[16] For simplicity, we use the optical $A_{2u}$ eigenmode of the unstrained system, even though under (110) strain this mode mixes with two $B_{1u}$ modes.
[17] A. Antons, J. B. Neaton, K. M. Rabe, and D. Vanderbilt, Phys. Rev. B **71**, 024102 (2005).
[18] O. Diéguez, K. M. Rabe, and D. Vanderbilt, Phys. Rev. B **72**, 144101 (2005).
[19] E. Shojaee and M. R. Mohammadizadeh, J. Phys.: Condens. Matter **22**, 015401 (2009).